International Journal of Thermophysics, Vol. 22, No. 3, 2001

Use of IR Spectroscopy, X-Ray Diffraction, and Petrographic Analysis to Evaluate Structural Changes in Aluminophosphate Compositions at Creeping

U. Shayachmetov,[1,2] R. Shayachmetov,[1] and I. Dranca[3]

received June 26, 2000

The present study is an attempt to evaluate the structural changes observed in ceramic compositions based on aluminum oxide and phosphate H_3PO_4 binders at creeping using IR spectroscopy, X-ray diffraction, and pectrographic analysis. The study reports the dependence of structural changes on the composition of the compounds, the type of phosphate binder, the temperature of processing, and the test conditions at creeping. On the basis of the test results and the data obtained elsewhere [1–7], it is surmised that the deformation process of phosphate compositions at high temperatures and loads is connected with a change in the physicochemical characteristics of the material and, as a consequence, with a change in its structure. It is revealed that the mechanism of deformation of aluminophosphate material at creeping depends primarily on the change in the matrix structure that cements the grains of electrocorundum in the material.

KEY WORDS: aluminum phosphate composition; creeping; IR spectroscopy; petrographic analysis; X-ray diffraction.

1. INTRODUCTION

The chemical technology of phosphate materials is one of the new trends in the field of material study, the development of which has allowed the production of a wide range of effective materials based on the system oxide–metal–phosphate binder. Such systems are rewarding objects for

[1] State Enterprise "Bashkir Scientific Research and Design Institute for Industry of Building Materials," 9 Zorge Str., Ufa, Republic of Bashkortostan 450059, Russia.
[2] To whom correspondence should be addressed. E-mail: rusairu@ufanet.ru
[3] Guest scientist from the Institute of Chemistry of the Academy of Sciences of Moldova, Str. Academiei Nr. 3, Chisinau, MD-2028, Moldova.

0195-928X/01/0500-0979$19.50/0

research and development of fireproof materials and objects based on them. The use of the latter has considerably prolonged the service term of lining in heating installations [8].

Phosphate materials, as well as many other ceramic materials, are brittle, and yet at high temperatures, plastic deformation and sometimes even rapid destruction are observed. The peculiarities of such processes and high temperature creeping of ceramic materials are studied in detail elsewhere [1–7].

Alongside the study of the dependence of creeping on temperature, load, and reaction time, deformation processes of ceramic and fireproof materials have been studied. The dependence of deformation creeping processes on the types of chemical binding and elementary cell structure has been shown [5].

There are many data in the literature on the processes of hardening and structure formation of aluminophosphate materials studied by the use of IR spectroscopy [9–19, 21–24]. As far as the interaction of aluminum oxide with orthophosphoric acid is concerned, the data are numerous but contradictory [20, 22]. There is certain information on deformation at creeping of phosphate materials [21], but there are no literature data on the study of this process using physical chemistry.

The objective of the work reported here was to study the physicochemical processes of hardening and structure formation that occur in binding systems and compositions based on aluminum oxide and phosphate binder depending on the initial components in the compositions and the type and temperature of treatment of the binder, as well to study the structural changes after their high-temperature deformation at creeping by IR spectroscopy, X-ray diffraction, and petrographic analysis.

2. MEASUREMENTS

2.1. Specimens

To prepare samples of binders and compositions of different structures (according to Table I), the following were used as initial powder components: Al_2O_3, electrocorundum Nos. 50 and 6, and fine-ground unhydrated alumina (FGAN). As hardening liquid, 85% H_3PO_4 or aluminochromophosphate binder (ACPB), which is a solution of different aluminum and chromium phosphates with the common formula $Al_2O_3 \cdot xCr_2O_3 \cdot yP_2O_5 \cdot nH_2O$, was used. The samples were prepared as follows: dry components were mixed with the phosphate binder, and the samples were formed from the prepared mass and thermally treated at 300, 900, and 1500°C. Aluminophosphate samples which were preliminarily treated at 300°C were

additionally tested for creeping on a unit designed at State Enterprise "BashNIPIstrom" [21].

2.2. Procedure

Infrared (IR) absorption spectra of binders and compositions were obtained using an M-80 spectrophotometer (Germany). Samples were prepared by grinding in an agate mortar and mixing with Vaseline oil. The crystal solidification product content was defined on a DRON-3 diffractometer with Co–K_α radiation (iron filter). Petrographic analysis was conducted using an MIN-8 microscope.

3. RESULTS

To determine the character of structural changes in the compositions after their deformation at creeping, we analyzed primarily the processes of structure formation in viscous systems and compositions based on aluminum oxide and phosphate binder by heating the samples up to the above-mentioned temperatures.

3.1. The Al_2O_3–P_2O_5 System (Samples 2–4 in Table I)

Samples of the system were thermally treated at 300°C (sample 2). Due to the fact that there had been excess Al_2O_3 in the system (mole ratio, $Al_2O_3:H_3PO_4 = 5:1$), aluminum oxide did not react fully with orthophosphoric acid. It is shown that the greatest part of the samples consists of Al_2O_3 bound with orthophosphates. Absorption lines appear in the IR spectra at frequencies of 1150, 1120, 1085, 800, 747, and 725 cm^{-1}, as well as others that should be considered valency and deformation fluctuations ν(Al–O), ν(P–O), and δ(O–P–O) of groups characteristic of $AlPO_4$ combinations. At least some of the above-mentioned frequencies are proof of new bonds appearing in the composition of the binder conditioned by the interaction of Al_2O_3 with H_3PO_4. This fact is proved by the data from X-ray PD (powder diffraction) analysis: the diffractogram reveals the formation of $AlPO_4$ (○) according to ASTM 11-500 (curves 2; Figs. 3 and 4). This formation could be a different form of $AlPO_4$ (phosphate bands according to ASTM 20-45 are clearly visible, along with traces of phosphate according to ASTM 20-44). As is known [25], α-Al_2O_3 starts reacting with H_3PO_4 at 200 to 250°C, Al hydrocomplexes of the $Al_2(OH)_3PO_4$, $Al_3(OH)_6PO_4$ type being formed therein. IR spectrum 2 reveals absorption lines at frequencies of 3400 and 1635 cm^{-1} (curve 2; Fig. 1). These may well represent bands of hydrophosphates of the OH group. However, O–H zones at 3200

Table I. Compositions Tested and Relation of Main Oscillating Frequencies (cm^{-1}) Revealed in IR Absorption Spectra in Samples Based on Aluminum Oxide and Phosphate Bindings[a]

Sample No. (1)	Composition (2)	ν(OH), ν_{as}(OH), ν_s(OH) (Al_2O_3) (3)	δ(OH), M–OH, H_2O (Al_2O_3) (4)	ν(Al–O–Al), ν(O–Al–O), ν(P–O) ($AlPO_4$), berlinite (crystaballite) (5)	Al_2O_3 (6)	v(P–O–P) (7)	δ(Al–O–Al), δ(P–O–P) (Al_2O_3) (8)	$AlPO_4$, δ(P–O–P) (9)	δ(Al–O–Al) (Al_2O_3) (10)	ν(M–O), $AlPO_4$ (berlinite) (Al_2O_3) (11)	$[PO_4]^{3-}$ (12)	$AlPO_4$ (Al_2O_3) (13)	$[PO_4]^{3-}$ (14)
1	α-Al_2O_3	(3390 w.wi.)	(1595 w.wi)	(1090 s.wi.)	(780 b.)	—	(720 b.)	(639 m.)	(590 s.)	(448 m.)	—	(393 w.)	—
2	α-Al_2O_3 (100%), H_3PO_4 (24%) $T=300°C$	3400 w.wi.	1635 w.wi.	1150 b. 1120 b. 1070b.	800 b.	747 b.	725 b.	648 w. 614 w. —	511 b.	460 s. 450 s	400 b.	390 m. 384 w.	348 w.
3	Same composition $T=900°C$	3400 w.wi.	1600 w.wi.	1170 s. 1120 b. 1030 b.	800 b.	752 b.	730 b.	648 w. 644 b.	510 b	470 s. 465 s.	405 b.	392w. —	348 w. 324 b.
4	α-Al_2O_3 (100%), H_3PO_4 (24%) $T=1500°C$	3405 w.wi.	1630 w.wi.	1190 b. 1120 s. 1080 b.	800 b.	755 b.	728 w.	— 628 b.	544 b.	476 w.	403 b.	392 w. 384 w.	348 w.
5	e/c (50–35%), e/c (6–40%), FGAN (Al_2O_3) (25%), H_3PO_4 (12%) $T=300°C$	3400 w.wi.	1650 w.wi.	1160 b. 1100 s.wi. 1020 b.	805 m. 780 m.	749 b.	720 w.	650 w. 624 w. 592 w.	515 w.	460 w.	?	380 w.	340 w.
6	Same composition $T=900°C$	3405 w.	1630 w.wi.	1150 b. 1096 s.wi. 1020 b.	800 m. 780 m.	759 w.	725 w.	644 w. — 588 m.	515 w.	460 m.	396 w.	370 b.	348 w.
7	e/c (50–35%), e/c (6–40%), FGAN (25%), H_3PO_4 (12%) $T=1500°C$	3520 w.wi. 3410 w.wi.	—	1150 b. 1108 s.wi. 1060 b.	800 b. 782 m.	748 w.	722 w.	646 w. 604 w. —	512 m.	464 m.	398 w.	388 w. —	340 w.

8	Composition analogous to No. 5 Deformation under 0.2-MPa load by Standard 4070-83 Max $T = 1450°C$	3412 w.wi.	1640 w.wi.	1170 b. 1100 s.wi. 1040 b.	802 m. 782 m.	760 w.	731 w.	655 m. 645 m. 599 m.	512 b.	461 m. 451 m.	398 w.	386 w. 372 w.	350 w.
9	Same composition $T_c = 1300°C$ $\tau = 159.54$ h $\sigma = 0.6$ MPa	3400 w.wi.	—	1115 b. 1092 s. 1045 b.	798 m. 779 m.	750 b.	738 w.	695 w. 680 w. 646 m. 610 w. 590 m.	515 b.	460 m. 455 b. 420 b.	396 w.	388 w. 370 w.	348 w. 304 w.
10	Same composition $T_c = 1400°c$ $\tau = 28.50$ h $\sigma = 0.6$ MPa	3405 w.wi.	1660 w.wi.	1160 b. 1090 s.wi. 1025 b.	805 b. 782 m.	760 b.	730 w.	690 w. 660 b. 600 w. 590 w. 565 w. 532 b.	512 b.	465 m. 453 m. 430 b.	397 w. 388 m.	372 w.	344 w. 328 w. 314 w.
11	Same composition $T_c = 1500°c$ $\tau = 57$ h $\sigma = 0.6$ MPa	3540 w.wi. 3400 w.wi.	1655 w.wi. 1610 w.wi.	1150 b. 1085 s. 990 b.	805 m. 783 m.	751 b.	735 w.	696 w. 650 m. 604 w. 590 m. ?	512 w.	462 m. 435 m.	397 m.	388 m. 372 w.	345 w. 326 w. 312 b.
12	Same composition, ACPB instead of H_3PO_4 $T = 300°C$ $T_c = 1200°C$ $\tau = 47.40$ h $\sigma = 0.6$ MPa	3404 w.wi.	—	1110 b. 1091 s. 1062 b.	798 m. 780 m.	743 b.	722 w.	698 b. 670 w. 645 m. 610 w. 590 m.	514 w.	462 m. — 430 b.	398 w.	388 w. 372 w.	356 w.

[a] Band intensity: s., strong; m., medium; w., weak; wi., wide; b., bending. e/c—electrocorundum; FGAN—finely grated alumina, nonhydrated; ACPB—aluminochromophosphate binder; T—temperature of treatment; T_c—temperature of creeping test; τ—time of creeping test; σ—load at creeping.

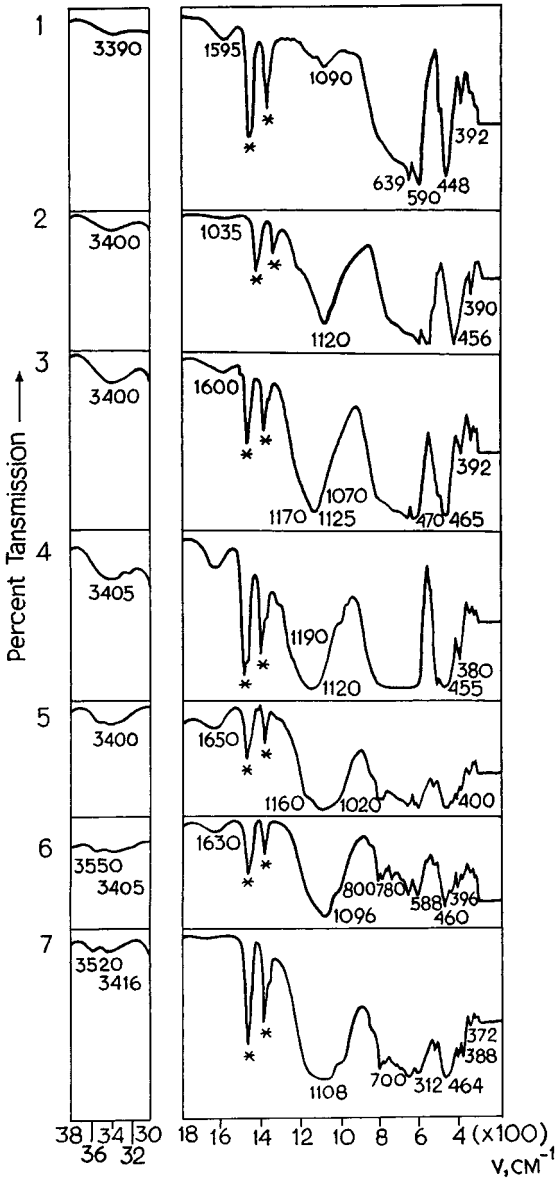

Fig. 1. IR absorption spectra of Al_2O_3 systems Al_2O_3–P_2O_5 and compositions (according to Table I) after thermal treatment: 2 and 5 at 300°C, 3 and 6 at 900°C, and 4 and 7 at 1500°C.

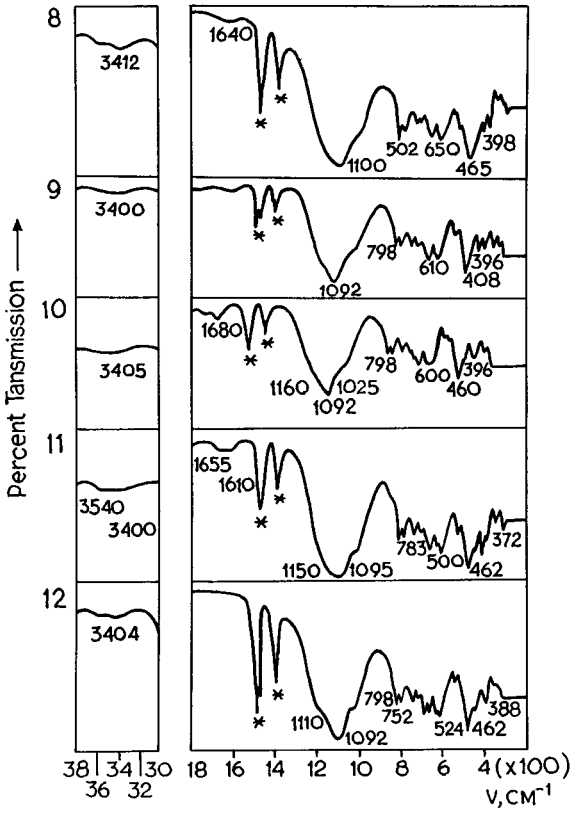

Fig. 2. IR absorption spectra of various compositions (according to Table I) after deformation under a load of 0.2 MPa with creeping at various temperatures: 8 at 1450°C, 9 at 1300°C, 10 at 1400°C, 11 at 1500°C, and 12 at 1200°C.

to 3500 and at 1600 to 1650 cm^{-1} are revealed in the spectra of practically all samples (see Table I and Fig. 2); in all probability these bands represent adsorbed water.

To determine the influence of the processing temperature on the physicochemical properties of the system, samples were analyzed at 900 and 1500°C (compositions 3 and 4 in Table I). Contour 3 in the IR spectrum (curve 3; Fig. 1) does not reveal marked differences from spectrum 2, which testifies to minor structural modifications; there was probably a redistribution of binding in valency and deformation oscillations ν(Al–O), ν(P–O), δ(Al–O–P), ν(P–O–P), etc., in $AlPO_4$, which results in consolidation of structural fragments and an increase in strength in the system. X-ray analysis (sample 3) reveals (curves 3; Figs. 3 and 4) an increase in the

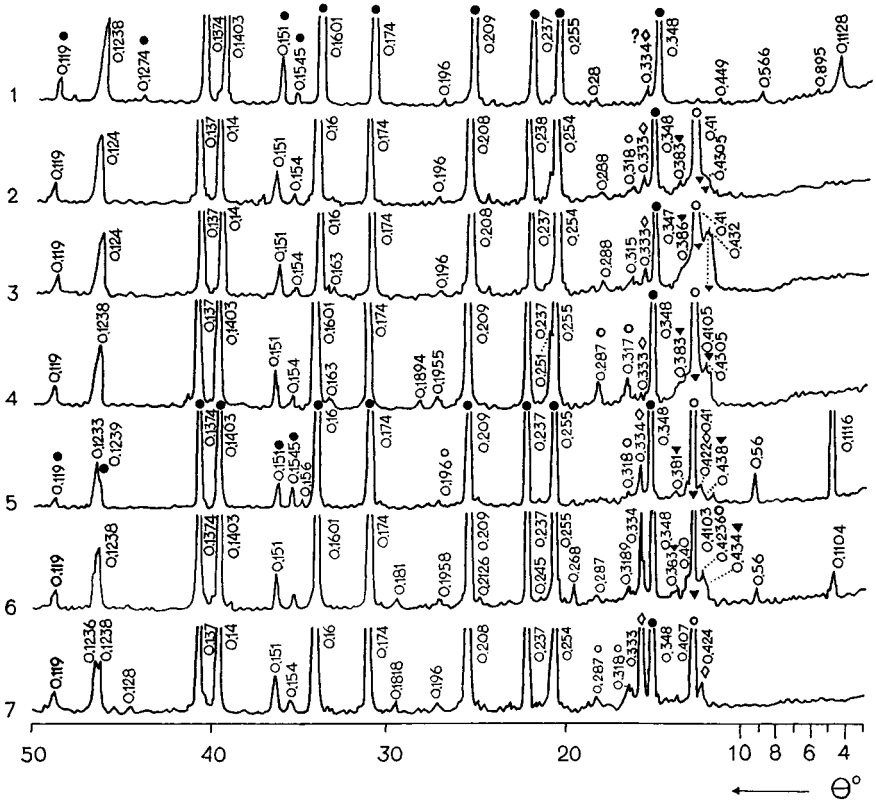

Fig. 3. X-ray diffractograms of Al_2O_3 and Al_2O_3–P_2O_5 at various compositions (according to Table I) after thermal treatment: 2 and 5 at 300°C, 3 and 6 at 900°C, and 4 and 7 at 1500°C. Main peaks: (●) α-Al_2O_3; (○) $AlPO_4$–phosphate; (▼) other phosphates; (◇) α-SiO_2 quartz.

intensity of $AlPO_4$ (○) X-ray reflexes (ASTM 11-500). This is visible in the 0.41-nm peak compared with the peak at 2. Reflexes of orthophosphates of other forms appear at 0.432 and 0.386 nm (▼) (ASTM 20-45 and 20-44). Quantitative change in the initial phosphate Al_2O_3 (●) and the one formed (○) is shown in Figs. 3 and 4 (curves 2 and 3). Thermal treatment at 1500°C (sample 4) results in further consolidation of binding ν(Al–O), ν(P–O), δ(Al–O–P), and others (curve 4; Fig. 1). This is especially noticeable in the range of $\sim$800 and $\sim$450 cm^{-1}. X-ray diffraction testifies (curves 4; Figs. 3 and 4) to the formation of $AlPO_4$ (○), with a high-intensity reflex at 0.4103 nm. With an increase in intensity, $AlPO_4$ (○) reflexes are preserved at 0.317, 0.287, 0.25, 0.1955, and 0.163 nm. At 0.1894 nm, a weak reflex of $AlPO_4$ (○) appears.

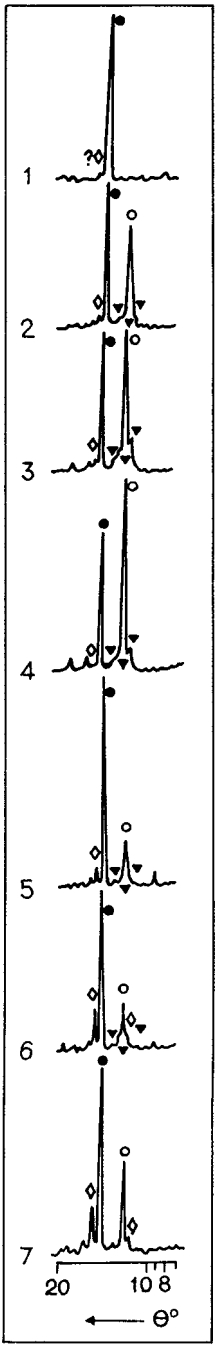

Fig. 4. Fragments of diffractogram patterns from Fig. 3 for Al_2O_3 and Al_2O_3–P_2O_5 with compositions according to Table I, after thermal treatment: 2 and 5 at 300°C, 3 and 6 at 900°C, and 4 and 7 at 1500°C. Main peaks: (●) α-Al_2O_3; (○) $AlPO_4$–phosphate; (▼) other phosphates; (◇) α-SiO_2 quartz.

3.2. Composition of Electrocorundum–Al_2O_3–P_2O_5 (Samples 5–7, in Table I)

The study of the binding system reveals the following. In IR spectra of the composition thermally processed at 300°C (sample 5) (curve 5; Fig. 1), absorption bands appear relating to valency and deformation oscillations ν(Al–O–Al) and δ(Al–O–Al) and, also, ν(P–O) and δ(P–O–P) at 1160, 1100, 1020, 805, 780, 749, 720, 650, 624, and 592 cm^{-1}, which pertain to the combination $AlPO_4$; this fact is confirmed by the peaks in the diffractograms (curves 5; Figs. 3 and 4) at 0.41, 0.308, and 0.19 nm (○) (ASTM 11-500). The weak-intensity peaks at 0.438, 0.422, and 0.381 nm (ASTM 20-45 and 20-44) correspond to other modifications of $AlPO_4$. Rather intensive peaks of aluminum oxide are preserved at 0.348, 0.209, 0.174, 0.16, 0.1403, and 0.1374 nm.

Thermal treatment at 900°C (sample 6) brings about the formation of the same phosphates as in system 3 but with more definite absorption bands at 800, 780, 759, 644, 588, 515, 460, and 396 cm^{-1} (curve 6; Fig. 1). This testifies to the establishment of a frame structure. X-ray plates (curve 6; Figs. 3 and 4) of the composition reveal new X-ray reflexes at 0.41, 0.318, 0.288, 0.250, and 0.163 nm, referring to $AlPO_4$ (○) (ASTM 11-500). Lines of other forms of $AlPO_4$ (▼) (ASTM 20-45 and 20-44) are detected, with significant (0.432 and 0.386 nm), as well as weak, SiO_2 lines (◇) accompanying initial components.

The IR spectrum over 1500°C (curve 7; Fig. 1) is characterized by absorption bands at the significant frequencies close to frequencies 5 and 6. However, modification of the intensities of frequencies in the range of 1100 and of 800 to 350 cm^{-1} relating to $AlPO_4$ testify to stabilization of the structural parameters of the given composition. The X-ray analysis data confirm these suppositions (curve 7; Figs. 3 and 4). An increase in intensity, however, is observed in the $AlPO_4$ peaks at 0.407, 0.318, 0.287, 0.2506, and 0.196 nm compared to frequencies 5 and 6. Other phosphates are not detected. The quantity of SiO_2 (◇) remained without modifications (0.424, 0.333, and 0.181 nm).

3.3. Composition of Electrocorundum–Al_2O_3–PB (Phosphate Binder) After Deformation at Creeping (Compounds 8–12 in Table I)

The physicochemical properties of the composition after deformation under a standard load of 0.2 MPa and creeping at different temperatures, loads, and curing times are studied on samples of compositions 8, 9, 10, 11, and 12.

Sample 8 is used to study the effect of deformation under a load of 0.2 MPa on the processes of structural changes occurring in the composition

at a temperature of 1450°C. Comparison of IR spectrum 8 (curve 8; Fig. 2) with spectra 5–7 testifies to minor modifications in the intensity of absorption bands in phosphates only and to the emergence of new absorption bands at frequencies of 655 and 451 cm^{-1}, relating to oscillations δ(P–O–P) and ν(M–O) of berlinite and crystoballite ($AlPO_4$) [20].

X-ray plate 8 reveals (curve 8; Figs. 5 and 6) lines at 0.406, 0.318, 0.287, 0.25, 0.1955, and 0.188 nm, relating to $AlPO_4$ (○) (ASTM 11-500), and lines at 0.43 and 0.6383 nm, due to other forms of phosphates (▼) (ASTM 20-45 and 20-44), whose intensity exceeds the intensity of similar peaks at 7. The peaks of SiO_2 (◇) at 0.424, 0.333, 0.245, 0.227, 0.2126, 0.1815, and 0.154 nm are preserved. A decrease in intensity of Al_2O_3 lines is observed therein.

In the IR spectrum of the composition above 1300°C (sample 9), there is no absorption band δ(O–H) in the range $\sim$1600 cm^{-1} (P–OH), and absorption bands relating to P–O–P binding characteristic of high-temperature phosphates have appeared. Based on the intensity of the X-ray peaks, their quantity equals that in samples 8 and 9; however, it is greater in 9 than in 7. Samples 8 and 9 also contain approximately equal quantities

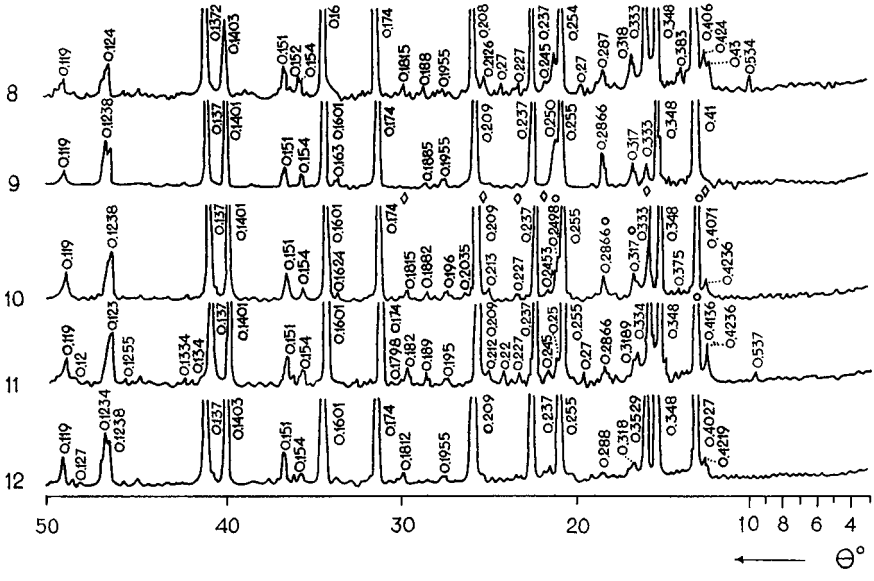

Fig. 5. Diffractograms of compositions (according to Table I) after deformation under a 0.2-MPa load and creeping at various temperatures: 8 at 1450°C, 9 at 1300°C, 10 at 1400°C, 11 at 1500°C, and 12 at 1200°C. Main peaks: (●) α-Al_2O_3; (○) $AlPO_4$–phosphate; (▼) other phosphates; (◇) α-SiO_2 quartz.

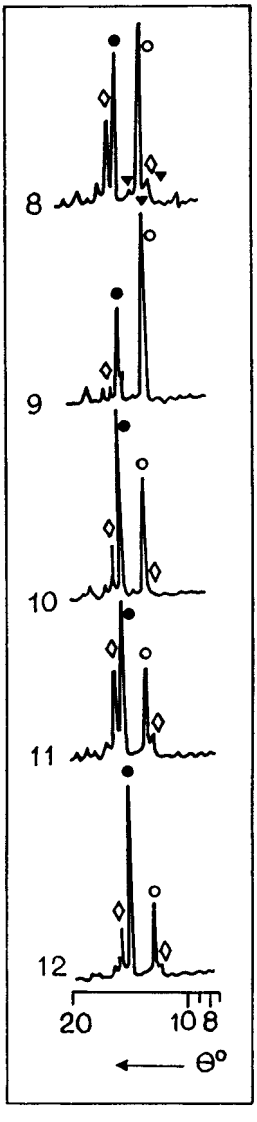

Fig. 6. Fragments of diffractogram patterns from Fig. 5 (according to Table I) after deformation under a 0.2-MPa load and creeping at various temperatures: 8 at 1450°C, 9 at 1300°C, 10 at 1400°C, 11 at 1500°C, and 12 at 1200°C. Main peaks: (●) α-Al_2O_3; (○) $AlPO_4$–phosphate; (▼) other phosphates; (◇) α-SiO_2 quartz.

of phosphates, however, there are more in 9 than in 7 due to the differences in temperatures and curing times under a load (curves 7–9; Figs. 5 and 6).

In IR spectrum 10, at an increase in temperature up to 1400°C, modification of the forms of absorption bands (curve 10; Fig. 2), displacement of certain frequencies, and modification of intensity in the range 800 to 350 cm^{-1} are observed. A decrease in intensity of the absorption band

at 1092 cm^{-1}, which is inherent in compositions containing the binder P–O, is observed at high temperatures. The decrease in intensity of bands in compounds with P–O binding has also been noted by other authors [22, 23]. A decrease in the quantity of phosphate in the given sample is observed in the X-ray PD (curve 10; Figs. 5 and 6). This is conditioned by the structural transformations occurring in the compositions due to their creeping within 28.5 h.

The IR spectrum of sample 11 (curve 11; Fig. 2) is characterized by a modification in the contour of absorption bands in the range 800 to 350 cm^{-1} compared to IR spectra 4, 9, and 10. The band at 990 cm^{-1} indicates the presence of P–O–P and P–O bindings; the decrease in their intensity testifies to a decrease in the quantity of phosphates and the formation of other (high-temperature) modifications of phosphates, crystaballite among them [22, 23]. By the method of differential thermal analysis (DTA), the transition of $AlPO_4$ (berlinite) $\rightarrow$ 1230°C $\rightarrow$ $AlPO_4$ (crystaballite) is observed in the system Al_2O_3–P_2O_5. Comparison of diffractograms of composition 11 (curves 11; Figs. 5 and 6) with those of compositions 4, 9, and 10 also testifies to a decrease in the quantity of phosphates at 11, the latter being connected with deformation processes at creeping.

Sample 12 is obtained with the use of ACPB. In IR spectra, new bands appear at 698, 645, and 430 cm^{-1}, relating to δ(P–O–P) and ν(M–O), which evidently refer to chromium phosphate. The IR contour testifies to the stability of the composition. Not very pronounced $AlPO_4$ ($\bigcirc$) reflexes at 0.4087, 0.328, 0.288, 0.25, and 0.1955 nm (ASTM 11-500) are discerned in the X-ray PD (curve 12; Figs. 5 and 6), as well as weak SiO_2 ($\diamond$) lines at 0.4219, 0.3329, and 0.1812 nm that create the frame of the composition cementing the particles of the filling.

3.4. Petrographic Analysis

This analysis is conducted with the help of an MIN-8 microscope in immersion liquid at a 320× magnification of samples without deformation (sample 7) and after deformation at creeping, the temperature being 1500°C (sample 11). Sample 11, when magnified, clearly reveals angular birefracting grains (Fig. 7), the largest grain being not more than 0.1 mm in diameter. The refractive indices of grains are very high (over 1.7), and birefraction equals 0.009.

Based on the data, all these grains are represented by corundum; this fact is also confirmed by diffractometric data. The smallest grains are not more than 0.003 to 0.005 mm in size. Among the grains there is a great amount (about 30 to 50% of the sample volume) of very thin dust consisting of the tiniest (up to 0.001-mm) grains, the optical constants of which

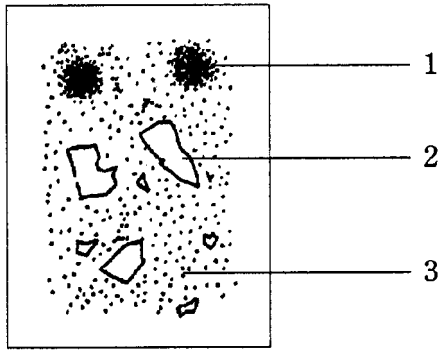

Fig. 7. Sample 4 in immersion liquid after deformation at creeping at 1500°C: (1) congestion of submicroscopic grains of the cementing mass; (2) large crystals from electrocorundum; (3) thin dispersion mass consisting, by X-ray data, of aluminum phosphate.

(indices of refraction, birefraction, etc.) do not lend themselves to determination even at the highest magnifying power of the microscope. Only from the X-ray PD data is it possible to surmise that they represent aluminum phosphate, some of them being finely divided alumina. More often than not these finest crystallites (grains) form semitranslucent balls, white in the reflected light. This thin dispersion mass demonstrates the mechanism of high-temperature creeping. The quantity of phosphates formed per unit area is higher in sample 7 than in sample 11, and the distances between particles of new formations, inert fillings, are shorter, this fact also being connected with the deformation of the composition.

4. CONCLUSIONS

The methods of IR spectroscopy, X-ray PD, and pectrographic analysis have been used to study binding systems and compositions based on aluminum oxide and phosphate binding (H_3PO_4 or ACPB). The influence of the compound composition, the type of binder, and the temperature of processing have been established, as well as the test conditions of the composition at creeping and their effect on the structural transformations and behavior at high temperatures.

The compositions, as the result of a long process of deformation at high temperatures and loads, reveal modifications of the physicochemical properties of the materials and, as a consequence, a change in their structures. In all probability, this determines the mechanism of the creeping

process that is caused by the change in the matrix (frame) cementing the grains of electrocorundum in the composition electrocorundum–Al_2O_3–phosphate binder (PB).

REFERENCES

1. A. G. Evans and T. G. Langdon, *Structural Ceramics* (Metallurgy, Moscow, 1980), p. 160.
2. G. N. Maslennikova, R. A. Mamaladse, S. Midzuta, and K. Koumoto, *Ceramic Materials* (Stroiizdat, Moscow, 1991), p. 96.
3. V. S. Bakunov, *Russ. J. Refract. Mat.* **12**:2 (1997).
3. D. N. Poluboiarinov and V. S. Bakunov, *Russ. J. Inorg. Mat.* **3**:374 (1965).
5. V. S. Bakunov and A. V. Beliakov, *Russ. J. Inorg. Mat.* **32**:243 (1996).
6. V. S. Bakunov and A. V. Beliakov, *Russ. J. Inorg. Mat.* **33**:1553 (1997).
7. E. M. Grishpun, Yu. E. Pivinskii, E. B. Rojkov, D. A. Dobrodon, I. A. Galenko, T. N. Kononova, *Russ. J. Refract. Mat. Tech. Ceram.* **3**:37 (2000).
8. L. G. Sudaskas. *Russ. J. Cement Appl.* **2–3**:34 (1999).
9. K. Nakamoto, *IR Spectra and CD Spectra of Inorganic and Co-ordination Compounds* (Mir, Moscow, 1991), p. 283.
10. K. Nakamoto, *Infrared Spectra of Inorganic and Co-ordination Compounds* (Mir, Moscow, 1966), p. 145.
11. V. V. Pechkovsky, R. Ia. Melnikova, E. D. Dziuba, I. I. Barannikova, and V. B. Nikanovich, *The Atlas of the Phosphate IR Spectra. Ortophosphates* (Nauka, Moscow, 1981), p. 143.
12. I. V. Tananaev, *The Atlas of the IR Spectra of Phosphates. Condencated Phosphates* (Nauka, Moscow, 1985), p. 114.
13. A. N. Lazarev, A. P. Mirgorodsky, and I. S. Ignatiev, *The Vibration Spectra of Complicated Oxides* (Nauka, Leningrad, 1975), p. 229.
14. E. N. Yurchenko, *Modern Vibrational Spectroscopy of Inorganic Compounds* (Nauka, Novosibirsk, 1990), p. 230.
15. L. D. Fredrickson, Jr., *Anal. Chem* **26**:1883 (1954).
16. J. M. Hunt, M. P. Wisherd, and L. C. Bonham, *Anal. Chem.* **22**:1478 (1950).
17. U. Sh. Shayachmetov, *The Compositions of Materials on the Basis of Si_3N_4 and Phosphate Binders* (Intermet Engineering, Moscow, 1999), p. 17.
18. A. A. Pashcenko, *New Cements* (Budivelnik, Kiev, 1979), p. 139.
19. J. Alamo and R. Roy, *Comm. Am. Ceram. Soc.* 80 (1984).
20. F. J. Gonzales and J. Halloran, *Am. Ceram. Soc. Bull.* **59**:727 (1980).
21. U. Sh. Shayachmetov, I. M. Valeev, K. A. Vasin, and R. S. Malikov, *Russ. J. Refract. Mat. Tech. Ceram.* **11**:21 (1999).
22. V. V. Gerasimov, *Inorganic Polymer Materials on the Basis of SIO_2 and Phosphorous* (Stroiizdat, Moscow, 1993), p. 131.
23. B. A. Kopeikin, *The Technology and Properties of Phosphate Materials* (Stroiizdat, Moscow, 1974), p. 17.
24. L. L. Vaniceva, O. V. Efremova, Iu. B. Materkin, and S. P. Shmitt-Fogelevich, *The Investigation and Application Methods of Refractory Materials in Metallurgy* (Moscow, 1983), p. 44.
25. J. R. Van Wazer, *Phosphorus and Its Compounds* (Inlit, Moscow, 1962), p. 26.